STUDIA UBB CHEMIA, LXIX, 2, 2024 (p. 81-96)
(RECOMMENDED CITATION)
DOI:10.24193/subbchem.2024.2.06

GOLD NANOPARTICLES SYNTHESIZED WITH NATURAL COMPOUNDS: ASSESMENT OF ANTIOXIDANT ACTIVITY AFTER *IN VITRO* DIGESTION

Dalina Diana ZUGRAVU (POP)[a], Teodora MOCAN[a], Andrei Vasile POP[b], Valentina MOROSAN[c*], Luminita DAVID[c], Simona Valeria CLICHICI[a]

ABSTRACT. Currently, gold nanoparticles (GNPs) are considered an ideal delivery system due to their physiological stability, high bioactivity, and controlled release of biological component. Our primary objective was to comprehend the behavior of gold nanoparticles obtained with specific natural compounds in the gastrointestinal tract. We investigated the conduct of GNPs synthesized with natural compounds from *Cornus mas* L. (GNPs-CM) or *Sambucus nigra* (GNPs-E) fruits, during the oral, gastric, and intestinal phases of the *in vitro* simulated gastrointestinal digestion. Additionally, we assessed their antioxidant capacity, phenolic content, and their potential to mitigate damages caused by nitro-oxidative stress after each phase of *in vitro* digestion. Results indicated that both GNPs-CM and GNPs-E maintained stability throughout simulated digestion, with some observed differences between them. Upon measuring antioxidant capacity, the GNPs-CM exhibited the lowest percentage of inhibition from hydrogen donor measurements (12.08%) after the simulated intestinal phase. Conversely, the GNPs-E displayed the highest inhibition percentage (65.3%) after the simulated oral phase. Concerning phenolic content, GNPs-CM showed a polyphenol content of 39.53 mg of gallic acid equivalents (GAE)/L, decreasing during gastrointestinal phases. GNPs-Eexhibited a polyphenol content of 100.99 mg GAE /l, also decreasing during gastrointestinal phases.

[a] *Department of Physiology, Faculty of Medicine, "Iuliu Haţieganu" University of Medicine and Pharmacy, 8, V. Babeş Str., 400012, Cluj-Napoca, Romania.*
[b] *2nd Medical Department, "Iuliu Haţieganu" University of Medicine and Pharmacy, Cluj-Napoca, Romania.*
[c] *Department of Chemistry, Faculty of Chemistry and Chemical Engineering, "Babeş-Bolyai" University, 11, A. Janos Str., 400028, Cluj-Napoca, Romania*
* *Valentina Moroşan valentina.morosan@ubbcluj.ro*

Keywords: *gold nanoparticles, simulated gastrointestinal digestion, Cornus mas L., Sambucus nigra L., nitro oxidative stress, antioxidant capacity, phenolic content.*

INTRODUCTION

Gold nanoparticles (GNPs) have emerged as a versatile and promising platform in the realm of nanotechnology for a multitude of applications, particularly in the field of drug delivery and therapeutics [1,2]. Their unique physicochemical properties, including size, shape, and surface characteristics, make them ideal candidates for functionalization with biocompatible ligands [3,4].

In recent years, the integration of natural compounds, derived from plants and recognized for their inherent biocompatibility and diverse biological activities, has significantly advanced the capabilities of GNPs in the context of medical applications. The gastrointestinal tract, encompassing the stomach, small intestine, and large intestine, represents a critical portal for the oral administration of drugs and therapeutic agents [3,4]. Effective delivery of these agents to specific sites within the gastrointestinal system relies on understanding and harnessing the behavior of nanoparticles in this dynamic and complex environment.

Factors including pH gradients, enzymatic activity, mucosal barriers, and transit times present substantial challenges to the efficacy of nanoparticle-based drug delivery systems. Consequently, there is a pronounced need for strategic approaches tailored to augment nanoparticle stability and bioavailability to overcome these challenges.

Joining nanoparticles and bioactive compounds promises to revolutionize the field of oral drug delivery. This offers opportunities for tailored therapies that exhibit enhanced bioavailability, reduced side effects, and improved patient compliance. It can contribute to the development of personalized medicine, where therapies can be fine-tuned to individual patient needs and conditions. For instance, a recent study demonstrated the synthesis of GNPs with different sizes and morphologies using a single LTCC-based microfluidic system for point-of-care use in personalized medicine. The study showed that depending on the temperature, residence time, and citrate concentration chosen during synthesis, a range of nanoparticle sizes and shapes were consistently produced. This indicates that the process could be suitable for the production of nanoparticles for personalized medicine [3].

The behavior of GNPs functionalized with natural compounds in the gastrointestinal tract opens a gateway to innovative approaches in pharmaceutical science, with far-reaching implications for drug delivery.

Nanotherapy is a cutting-edge therapeutic approach that uses nanoparticles to deliver drugs into specific targeted cells. The process is based on nanoparticles specific characteristics including their size, core composition, shape and surface functionalization. Due to their capacity to cross numerous biological barriers and release a therapeutic load in the ideal dosage range, nanoparticles drug delivery systems (5-250 nm) have the potential to revolutionize current disease therapies. [5]

Nanostructured coatings and surface tailoring can be applied to the outside of a matrix to improve or enhance its efficiency. Gold nanoparticles can deliver a variety of drug molecules, from tiny ones to large biomolecules like peptides, proteins, or nucleic acids like DNA or RNA. Numerous molecules with the proper functional groups could be used to functionalize gold nanoparticles. The synthesis of GNPs is achieved with nontoxic effects, obtaining unique biological, physiochemical, and optical features [6,7].

In various *in vitro* and *in vivo* experiments, multiple studies have consistently observed no adverse biological effects associated with GNPs. It is noteworthy that certain observed effects are attributed to compounds linked to the GNPs, rather than the GNPs themselves. Recent research has showcased the anti-inflammatory effects of GNPs functionalized with natural compounds in mice, evidencing a reduction in IL-6 mRNA and TNF-α levels [8]. Investigations on gold nanoparticles (GNPs) have underscored the significance of composition, surface derivatization, charge, size, and shape in determining their interaction with biological systems. The toxicity of GNPs is influenced by surface functionalization, necessitating individual evaluation of each unique nanomaterial. The application of DNA-GNPs for genetic regulation and amine-functionalized conjugates for drug delivery exemplify the potential of GNPs, with toxicity lower than polymer delivery systems. The field of functionalized gold nanoconjugates continues to evolve, offering potential applications in biology and medicine [9].

Belonging to the Cornaceae family, *Cornus mas* is native to South-West Asia and South-East Europe. Employed in traditional medicine for over a millennium, it has been particularly utilized for addressing digestive disorders [10]. The therapeutic potential of *Cornus mas* is substantial, primarily owing to its remarkable antioxidant capabilities derived from a rich composition of phytochemical compounds [11,12]. Noteworthy among these are significant amounts of phenolic compounds such as caffeic acid, ellagic acid, anthocyanins, and flavonoids [13]. *Cornus mas* finds widespread application in treating various conditions, including gastrointestinal disorders, diabetes, malaria,

inflammatory processes, and obesity [14]. The consumption of CM is deemed safe with no reported side effects, as indicated by toxicity studies. However, before categorizing CM as an herbal drug, it is essential to conduct extensive toxicity research and evaluate the effects of high doses [15].

Given its positive impact on gastrointestinal disorders coupled with its antioxidant and anti-inflammatory attributes, we explored the potential synergies by associating *Cornus mas* phytocomponents with GNPs. The aim was to leverage the combined effects of natural compounds of *Cornus mas* fruits and GNPs. Building on this premise, we investigated the behavior of nanoparticles synthesized with *Cornus mas* fruit extract in the digestive tract [16].

Elderberry, scientifically known as *Sambucus nigra* L., is a prevalent species within the Caprifoliaceae family, thriving in sunlit areas across Europe, Asia, North Africa, and the USA. The concentrated presence of health beneficial compounds in elderberries suggests that their consumption may contribute to the prevention of various degenerative illnesses, including diabetes, cancer, inflammatory diseases, and cardiovascular conditions [17]. *Sambucus nigra* assumes significance in medicine due to its chemical composition, encompassing phenolic acids, essential oils, flavonoids, free fatty acids, glycosides, vitamins, carotenoids, and minerals [18].

Phenolic acids represent key metabolites found in elderberry flowers and fruits, displaying significant antioxidant activities both *in vivo* and *in vitro* [19]. These compounds exhibit diverse biological effects, including antiviral, anti-carcinogenic, vaso-protective, anti-allergic, and anti-inflammatory properties [20]. Noteworthy for their antibacterial and antiproliferative activities, these compounds contribute to the antioxidant role of *Sambucus nigra* compounds. Given its antiproliferative and antioxidant properties, *Sambucus nigra* fruits emerged as a suitable candidate for our study [21,22].

To effectively apply gold nanoparticles in the real biological context, a deeper understanding of the potential interactions between biomolecules and gold nanoparticle materials, both *in vivo* and *in vitro*, is imperative. A key focus of research involves exploring the interactions among various biomolecules and nanoparticle materials. These interactions play a pivotal role in influencing the biological activity, stability, outcomes, and toxicity of nanoparticle bioconjugate materials in both *in vitro* and *in vivo* settings [23].

Aim: Our primary objective was to elucidate the behaviour of gold nanoparticles synthesized with specific natural compounds within the gastrointestinal tract. We investigated the conduct of GNPs obtained with either *Cornus mas* L. or *Sambucus nigra* fruits extracts throughout the oral, gastric, and intestinal phases, employing simulated gastrointestinal fluids. The secondary aim was to evaluate their antioxidant capacity following each phase of *in vitro* digestion, along with assessing their phenolic content.

RESULTS AND DISCUSSION

I. Synthesis and characterization of gold nanoparticles

The synthesis of gold nanoparticles was achieved by reducing gold ions from the tetrachloroauric acid by natural compounds from *Cornus mas* and *Sambucus nigra* fruits extracts.

The development of the gold ions reduction reaction and the formation of colloidal gold was spectroscopically monitored. In both cases, the UV-Vis spectrum of the biosynthesized gold nanoparticles exhibits the characteristic SPR band for metallic gold: λ_{max} = 541 nm for GNPs-CM and 543 nm for GNPs-E (Figure 1).

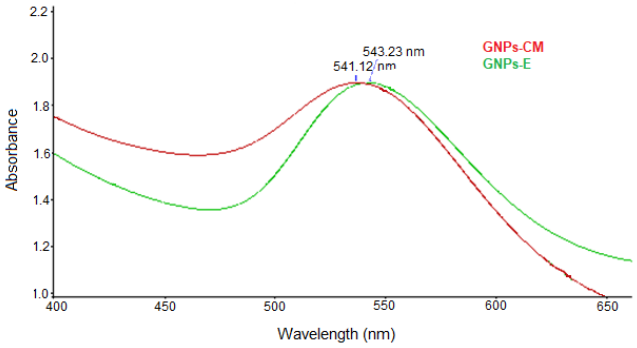

Figure 1. UV-Vis spectra of green synthesized gold nanoparticles

Transmission electron microscopy was used to determine the size and shape of newly obtained gold nanoparticles which, according to TEM images (Figure 2), were almost spherical, with a mean diameter of 42 ± 2.42 nm (GNPs-CM) and 44 ± 1.48 nm (GNPs-E), respectively.

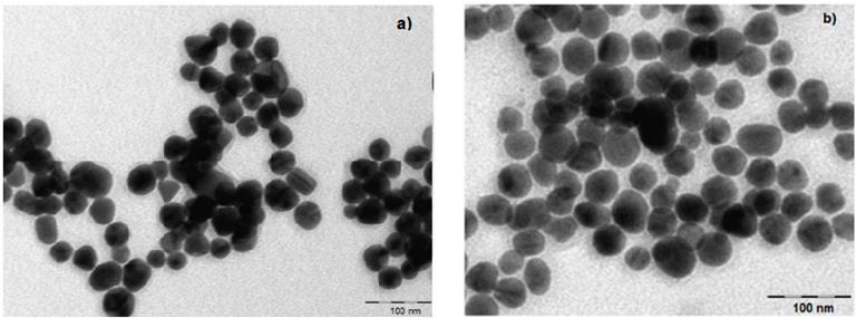

Figure 2. TEM images of: a) GNPs-CM; b) GNPs-E

II. In-vitro simulation

II.1. Macroscopic observation

Phytoreduced nanomaterial GNPs-CM demonstrated physical stability across all three phases of *in vitro* digestion. No color shifts were observed across phases. (Figure 3) No visible sediment, as a mark of particle aggregation, could be detected following the individual phases of *in vitro* simulated digestion for GNPs-CM / GNPs-E. Progressive dilution protocol resulted in decreased color intensity as the experiment moved toward the last step. However, color range remained stable, no significant red of blue shift could be observed across phases.

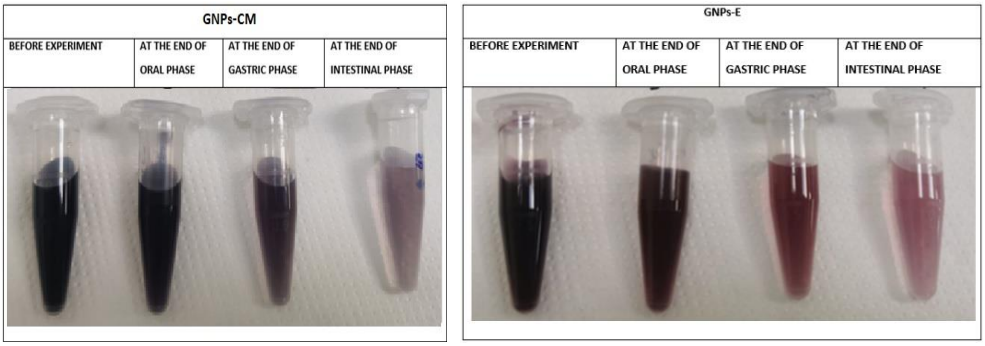

Figure 3. Macroscopic aspect of GNPs-CM and GNPs-Esolutions at various steps of *in vitro* gastrointestinal transit simulation.

II.2. UV-Vis Spectroscopy Evaluation

The UV-Vis spectra demonstrate stability for both structures across the digestive transit simulation (Figure 4 and 5).

II.3. Dynamic Light Scattering

Dynamic Light Scattering (DLS) analysis before the digestive *in vitro* simulation as well as at the end of each phase reveals a polydispersed solution. The pre-digestion sample of GNPs-CM presented a polydispersity index (PdI): 0.696, Peak 1: 294.9 ±67.20 nm cumulating 70.9 % of particles, Peak 2: 76.76±12.76 nm cumulating 29.1%. Following the oral phase, the obtained values were: PdI: 0.411, Peak 1: 514.0±99.56 nm cumulating 85.6% of nanostructures, Peak 2: 182.2±35.39 nm joining 14.4% of nanoparticles. At the end of the gastric phase, we obtained PdI: 0.488, Peak 1: 288.8± 165.8

nm cumulating 98.7% of nanostructures, Peak 2: 5289± 411.3 nm for 1.3% of nanoparticles. At the end of the experiment, PdI: 0.572, the initial Peak 1: 125.2± 39.35nm is found as cumulating 62.8%, Peak 2: 457.8± 124.5 nm appeared cumulating 27.7%, and Peak 3: 24.03± 4.42 nm cumulating 7.8% of nanoparticles. The complete disappearance of the smaller population, visible before the intestinal phase was observed. (Figure 5a).

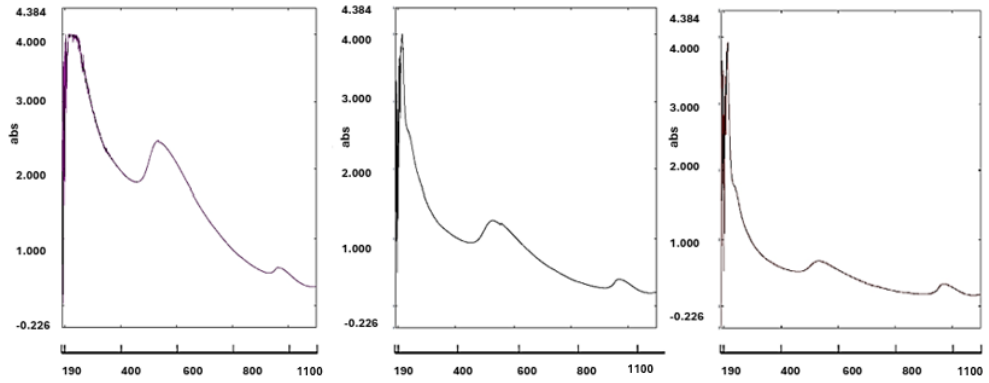

a)

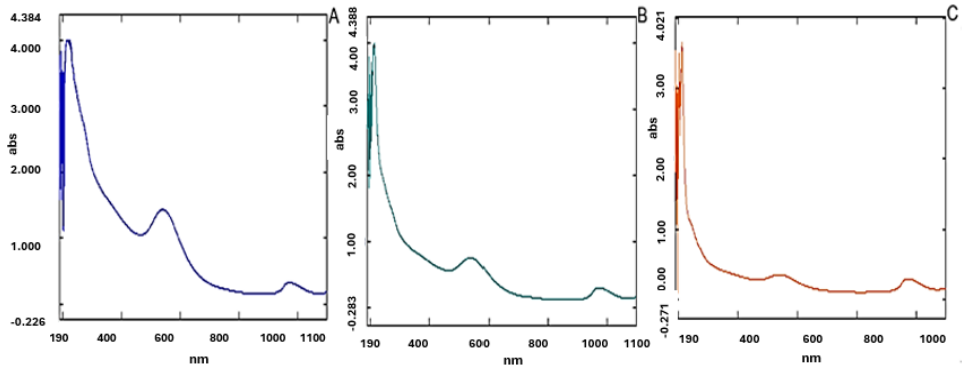

b)

Figure 4. UV-VIS spectra of a) GNPs-CM and b) GNPs-E samples resulting from *in vitro* digestive exposure steps. A. Sample at the end of SSF exposure. B. Sample at the end of SSF and SGF exposure steps, in respective order. C. Sample at the end of SSF, SGF and SIF exposure steps, in respective order.

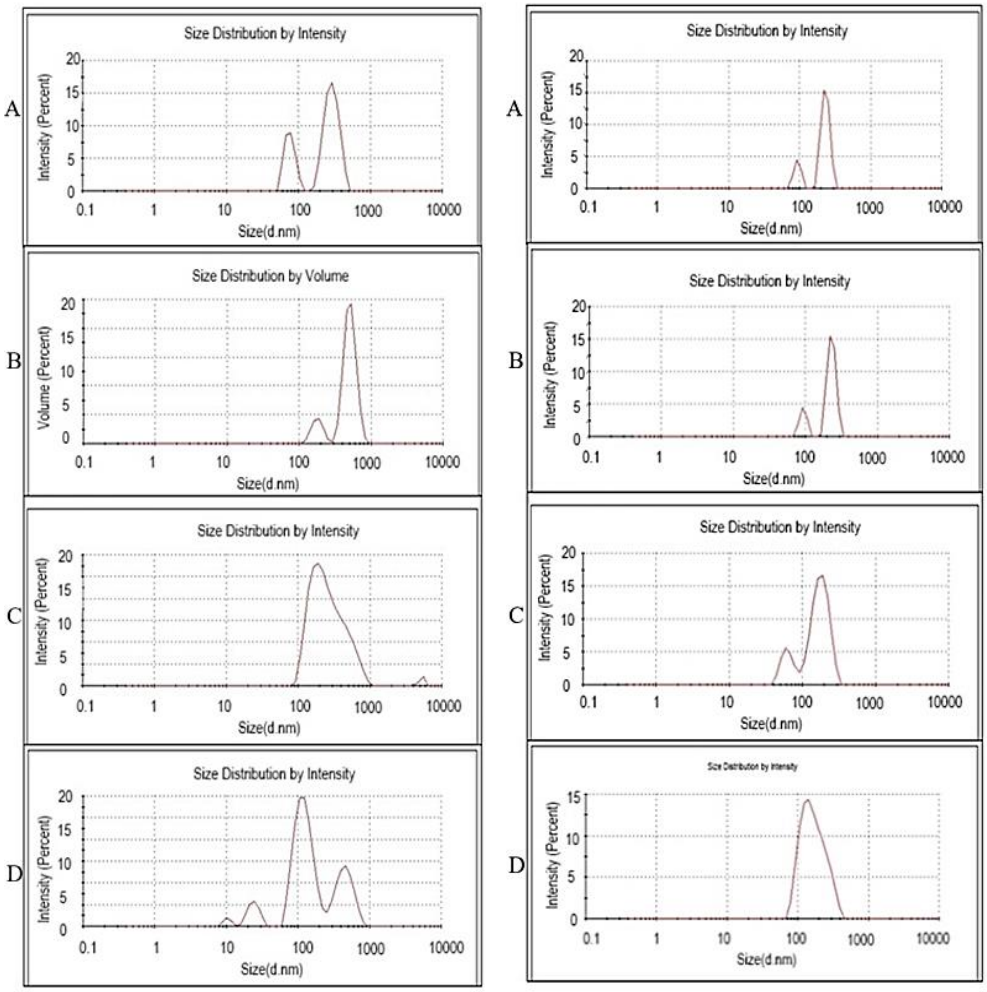

Figure 5. DLS analysis of samples following exposure of: a) GNPs-CM and b) GNPs-E to digestive simulated fluids. A. Sample before exposure to simulated digestive fluids. B. Sample at the end of SSF exposure. C. Sample at the end of SSF and SGF exposure steps, in respective order. D. Sample at the end of SSF, SGF and SIF exposure steps, in respective order.

For GNPs-E, DLS analyses before the digestive *in vitro* simulation as well as after each phase of the *in vitro* digestion process reveal a polydispersed solution. A small population of nanoparticles is also visible.

Control sample returned a polydispersity index (PdI): 0.314, Peak 1: 153.1± 36.30 nm cumulating 98.1% of particles. Following the oral phase values remained similar: PdI: 0.411, Peak 1: 233.4± 31.06 nm cumulating 82.1% of nanostructures, Peak 2: 93.5± 9.52nm nm joining 17.9% of nanoparticles. At the end of gastric phase, we have obtained PdI: 0.488, Peak 1: 180.2± 47.18 nm cumulating 80.1% of nanostructures, Peak 2: 64.08± 13.13nm for 19.9% of nanoparticles. Interestingly, the last intestinal step in digestive *in vitro* simulation induced a modification of the hydrodynamic diameter. At the end of the experiment, PdI: 0.572, the initial Peak 1: 174.6±69.66nm is found as cumulating 100%. Disappearance of the smaller population, visible before the intestinal phase was also observed at the end of the experiment (Figure 5b).

II.4. Assessment of Antioxidant Capacity through DPPH Inhibition

After measuring the antioxidant capacity, the lowest percentage of inhibition of DPPH from the measurements of hydrogen donors was presented by the GNPs-CM (12.08%) after simulated intestinal phase, followed by GNPs-CM exposed at simulated gastric phase (13.76%) and GNPs-CM exposed to simulated salivary fluids (20.79%) (Figure 8). It was observed that the GNPs-E after simulated oral digestion presented the highest inhibition percentage (65.3%), followed by GNPS-E before digestion (50.5%) and GNPs-E after simulated gastric phase (33.39%). A close percentage of inhibition was determined for both GNPs-CM (21.68%) and GNPs-E(22.57%) exposed at simulated intestinal fluid (Figure 6).

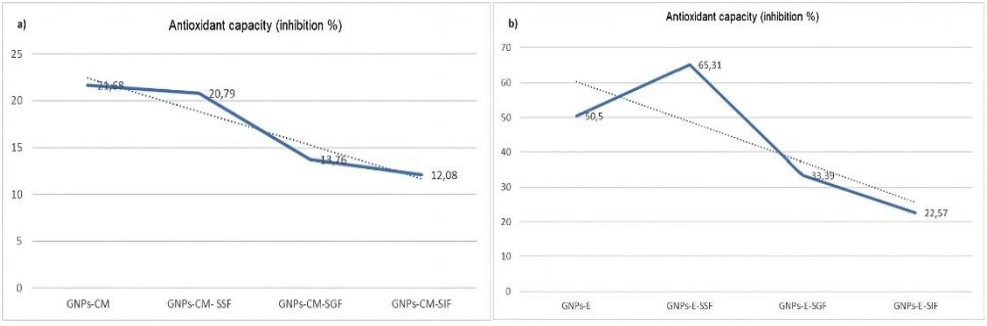

Figure 6. Inhibition percentage for: a) GNPs-CM and b) GNPs-E during gastrointestinal phases; GNPSs-CM, GNPs-E= gold nanoparticles before digestion; GNPs-CM-SSF, GNPs-E-SSF = gold nanoparticles exposed to simulated salivary fluid; GNPs-CM-SGF, GNPs-E-SSF = gold nanoparticles after simulated gastric digestion; GNPs-CM-SIF, GNPs-E-SSF = gold nanoparticles exposed to simulated intestinal fluid

II.5. Polyphenolic content

Regarding the polyphenolic content, our results showed that GNPS-CM have a polyphenol content in the amount of 39.53 mg of gallic acid equivalents (GAE)/L, this amount decreasing during the gastrointestinal phases, after exposure at SSF being 24.25 mg GAE/L, after exposure at SGF being 18.65 mg GAE/L and after the final phase of digestion being 8.43 mg GAE/L (Figure 7).

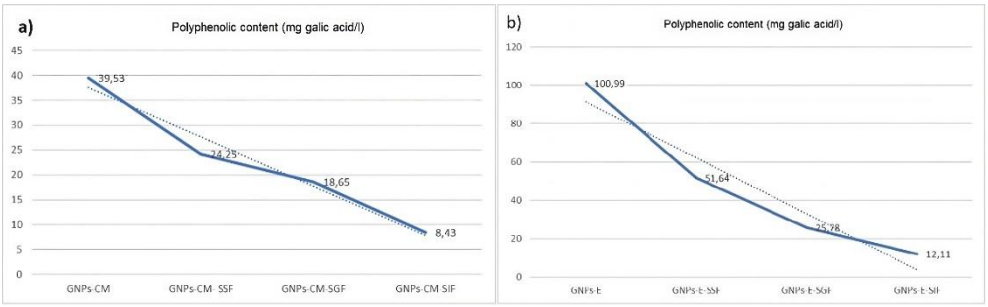

Figure 7. Phenolic content of: a) GNPs-CM and b) GNPs-Eduring gastrointestinal phases.

As far as GNPs-E is concerned, it has a polyphenol content of 100.99 mg gallic acid equivalents/L, also decreasing during the gastrointestinal phases: SSF 51.64 mg GAE/L, SGF 25.78 mg GAE/L, and SIF 12.11 mg GAE/L.

Both GNPs-CM and GNPs-E were stable across simulated digestion. However, differences were observed between the two. GNPs-E demonstrates stable interactions between natural compounds from the fruit extract and metallic component. It furthermore slightly increased the hydrodynamic diameter of the particles along the experiment, up to the end of the intestinal phase. Detachment of natural compounds from the metallic core is observed in the gastric stage. End-experiment sizes of particles are slightly larger than the pre-experiment dimensions. All data suggest a stabilization and reattachment of extract molecules in the intestinal phase, following a previous separation during the gastric phase.

By contrast, GNPs-CM nanoparticles transiently increase their dimension during the salivary phase, most likely by attachment of amylase onto the surface of the metallic core. Next, the gastric phase is associated with a decrease in hydrodynamic diameter, as a sign of detachment of extract's biomolecules from the nanoparticles' surface. This aspect is similarly present in most

nanoparticles (98.7%). Following this step, the intestinal phase induces a different result. Multiple particle populations are seen at the end of the experiment. A distinct fraction of components has small dimensions, the aspect suggesting detachment of extract molecules from the metallic surface of nanoparticles.

Up to now, we have found *in vitro* digestive studies only on other nanoparticles (NPs) such as Ag and ZnO NPs exposed to the salivary fluid. A study conducted by Pokrowiecki et al. [24] showed that this type of nanoparticles, when placed in salivary fluid for over 24 hours, presented high destabilization due to the salivary composition. In our study the exposure to salivary fluid was for 2 minutes to avoid the long persistence of GNPS in the salivary fluid. In the study conducted by Pokrowiecki et al., when nanoparticles were introduced into the artificial saliva, they agglomerated rapidly, which is different from our study where this agglomeration of gold nanoparticles was not present [24].

To the best of our knowledge, the assessment of GNPs-CM in the gastrointestinal tract has not been previously studied. Although the behavior GNPs in gastric condition, or in intestinal fluid has been reported, the complexity of *in vitro* digestive transit simulation could provide valuable information regarding GNPs stability and behavior in oral administration applications [25].
The results of our study align with existing literature, showing a high total phenolic content in *Sambucus nigra* (ranging from 91.09 to 746.63 mg gallic acid/l) [26].

CONCLUSION

Good stability of investigated GNPs along exposure to different simulated digestive fluids was observed on the analyzed nanoparticles. Along the transit, the gold nanoparticles have the tendency to additionally attach *Cornus mas* and *Sambucus nigra* functional moieties on their surface, increasing their diameter while proportionally reducing the free *Cornus mas* and *Sambucus nigra* molecule fraction in the solution. The significantly improved hydrodynamic diameter homogeneity of solution at the end of the experiment represents a consequence of this phenomena, providing the evidence for a good potential of the nanomaterial in human application with involving oral administration. Our study showed that *Sambucus nigra* contained more

abundant phenolic compounds than *Cornus mas*. This study has shown that elderberries can be an important source of antioxidant.

EXPERIMENTAL SECTION

I. Synthesis of nanoparticles

Due to their high content in antioxidant compounds, the fruits of *Cornus mas* L. and *Sambucus nigra* L. fruits are valuable sources of reducing agents of the gold ions and of capping agents of the obtained gold nanoparticles. The green synthesis of gold nanoparticles was achieved according to the protocol applied by Moldovan and co-workers [27]. Thus, the fruit extract was mixed under stirring with boiling 1 mM solution of tetrachloroauric acid in a 1:4 (vol/vol) ratio. After 15-30 minutes, the mixture's colour changed from red to purple, indicating the formation of colloidal gold. The *Cornus mas* fruit extract was prepared according to the method of Baldea et al. [28]. Obtaining the fruit extract of *Sambucus nigra* followed the same procedure, except for the amount of fruits used, which was twice as low as in the case of *Cornus mas* fruits.

II. Characterization of metallic nanoparticles

The monitoring of the formation of gold nanoparticles was achieved by UV-Vis spectroscopy (using a Perkin Elmer Lambda 25 double beam spectrometer), while transmission electron microscopy (TEM), was used to investigate their shape and size (by a Hitachi Automatic H-7650 microscope operated at 120 kV).

III. In vitro digestion

Gold nanoparticles obtained with *Cornus mas* (GNPs-CM] or with *Sambucus nigra* (GNPs-E) fruits extracts have been subjected to preliminary testing using *in vitro* digestive method, according to protocol developed by Minekus and co-workers [29].

Oral phase: Simulated salivary fluid (SSF) was prepared as to contain standard electrolyte and enzyme concentration (K^+:18.8 mmol/L, Na^+:13.6 mmol/L, Cl^-:19.5 mmol/L, $H_2PO_4^-$: 3.7 mmol/L, HCO_3^-, CO_3^{2-}: 13.7 mmol/L, Mg^{2+}: 0.15 mmol/L, NH_4^+: 0.12 mmol/L, $Ca2^+$: 1.5 mmol/L, amylase: 75 U/mL). The final pH of SSF was 7. According to the protocol, the nanomaterial was mixed with SFF using a 50:50 (vol/vol) ratio, for a period of 2 minutes incubation (37°C).

Gastric phase: Simulated gastric fluid (SGF) was prepared according to protocol. The electrolyte and enzymatic content of SGF included: K^+: 7.8 mmol/L, Na^+: 72.2 mmol/L, Cl^-: 70.2 mmol/L, $H_2PO_4^-$: 0.9 mmol/L, HCO_3^-, CO_3^{2-}: 25.5 mmol/L, Mg^{2+}: 0.1 mmol/L, NH_4^+: 1.0 mmol/L, Ca^{2+}: 0.15 mmol/L, pepsin: 2000 U/mL). The pH of final SGF solution was 3. The gastric phase included the collection of the mixture resulting from previous step and mixing it with SGF using a 50:50 (vol/vol) ratio. Incubation of 2 hours at 37°C was allowed.

Intestinal phase: Simulated intestinal fluid (SIF) was prepared. The solution presented a pH of 7 and included electrolytes such as: K^+: 7.6 mmol/L, Na^+: 123.4 mmol/L, Cl-: 55.5 mmol/L, $H_2PO_4^-$: 0.8 mmol/L, HCO_3^-, CO_3^{2-}: 85 mmol/L, Mg^{2+}: 0.33 mmol/L, Ca^{2+}: 0.6 mmol/L. Also, individual enzymes were added to the solution: trypsin: 100 U/mL, chymotrypsin: 25 U/mL, pancreatic lipase: 2000 U/mL, colipase (2:1 molar ratio with lipase), pancreatic amylase 200U/mL, bile (10mM). The intestinal phase included collection of aqueous mixture resulted from gastric phase and mixing it with SIF using 50:50 (vol/vol) ratio. Incubation of 2 hours at 37°C was allowed to the resulting mixture.

III.1 Evaluation of fluids obtained after each phase of in vitro digestion.

After each phase the samples were analyzed using macroscopical observation (color, sediment), spectral analysis (UV-Vis spectroscopy), and by assessing hydrodynamic diameter (DLS).

III.1.1*. Macroscopic observation*

Color changes and the presence of observable sediment at the bottom of containers were evaluated.

III.1.2. *UV-Vis spectroscopy*

UV-Vis spectra were recorded using a Shimadzu UV-1800® instrument. Samples were subjected to dilution (1:10 vol/vol) prior to the measurements. Normalization of spectra was performed using OriginLab software® 7.0.

III.1.3 *Dynamic Light Scattering*

The hydrodynamic diameter was measured using dynamic light scattering technique, using a Malvern Zetasizer NanoZS90 (Malvern, Instruments, Westborough, UK) equipment. Measurements were performed at a 90° diffraction angle, 25°C temperature, 0.2 refraction index, and 3.320 absorbance.

III.1.4. *Assessment of antioxidant capacity of fluids obtained after each phase of in vitro digestion.*

The measurement of hydrogen donor capacity is based on the reduction of the stable radical 1,1-diphenyl-picrylhydrazyl (DPPH) by a number of nonenzymatic antioxidants such as glutathione, tocopherol, ascorbic acid. This reduction can be tracked by changing color from purple to pale yellow, monitored by changes of samples absorbance at 520nm.

Samples are diluted with phosphate buffer 10 mM, pH 7,4. Then 0,5 ml of the solution 0.1mM of DPPH was added left for 30 min at room temperature and the absorbance against the blanks was read. Blanks consist of samples treated in the same way as samples, but in which absolute methanol has been added instead of DPPH solution. In parallel, the absorbance of some control samples that do not contain serum, but an appropriate volume of phosphate buffer is determined. Hydrogen donor capacity is expressed as Inhibition % in relation to the control samples according to the following calculation formula:
Inhibition% = [(Control absorbance – Serum sample absorbance) / Control absorbance] x 100 [30].

III.1.5. *Polyphenolic content assessment*

Folin-Ciocalteu method [31] was used to determine the total phenolic content. 3 mL Folin-Ciocalteu reagent was mixed with a sample of 0,5 mL of the diluted sample and permitted to react for 5 min in the dark, adding then 2,4 mL of 0.7 M Na_2CO_3 solution. The solution was incubated 2h in the dark at room temperature (22°C).

The absorbance of the mixture was measured with UV-Vis spectrophotometer Perkin Elmer Lambda 25 (Perkin Elmer, Shelton, CT USA) on a double beam against a blank sample. Using the gallic acid (GA) standard curve (0-100mg/mL), the total phenolic content of the extract is expressed as mg GA equivalents/mL. [32]

ACKNOWLEDGMENTS

This project was supported by a PhD research project (PCD nr 2462/66/17.01.2020) offered by Iuliu Hatieganu University of Medicine and Pharmacy, Cluj-Napoca, Romania

REFERENCES

1. Saha S, Xiong X, Chakraborty PK, Shameer K, Arvizo RR, Kudgus RA, Dwivedi SK, Hossen MN, Gillies EM, Robertson JD, Dudley JT, Urrutia RA, Postier RG, Bhattacharya R, Mukherjee P, *ACS Nano*, **2016**, *10*(12), 10636–10651.
2. V. H. Nguyen, B. J. Lee, *Int. J. Nanomedicine*, **2017**, *12*, 3137–3151.
3. Dalibera, NC, Oliveira AF, Azzoni AR, *Microfluid Nanofluid*, **2023,** 27, 56.
4. C. Li, D. Li, G. Wan, J. Xu, W. Hou, *Nanoscale Res. Lett*., **2011**, *6*, 1–10.
5. Alexis F, Pridgen E, Molnar LK, Farokhzad OC. *Mol. Pharm*. **2008**, *1*, 505–515.

6. Ielo I, Rando G, Giacobello F, Sfameni S, Castellano A, Galletta M, Drommi D, Rosace G, Plutino MR*, Molecules*. **2021**, *26*, 5823.
7. Kolanthai E, Fu Y, Kumar U, Babu B, Venkatesan AK, Liechty KW, Seal S. *Wiley Interdiscip Rev Nanomed Nanobiotechnol*.**2022**, *14*, e1741.
8. Chen H, Dorrigan A, Saad S, Hare DJ, Cortie MB, Valenzuela SM, *PLoS One*. **2013**, *8*, e58208.
9. Giljohann DA, Seferos DS, Daniel WL, Massich MD, Patel PC, Mirkin CA*. Angew. Chem. Int. Ed*. **2010**, *49*, 3280–94.
10. Dinda B, Kyriakopoulos AM, Dinda S, Zoumpourlis V, Thomaidis NS, Velegraki A, Markopoulos C, Dinda M. *J Ethnopharmacol*. **2016**, *193*, 70–90.
11. Moldovan B, David L. *Foods*, **2020**, *9(9)*, 1266.
12. Moldovan B, David L, *Mini-Rev. Org. Chem.* **2017**, 14, 489-495.
13. Jurca T, Baldea I, Filip GA, Olteanu D, Clichici S, Pallag A, Vicas L, Marian E, Micle O, Muresan M. *J. Physiol. Pharmaco*l. **2020**, 71.
14. Mikaili P, Koohirostamkolaei M, Babaeimarzangou SS, Aghajanshakeri S, Moloudizargari M, Gamchi NS, Toloomoghaddam S. *J. Pharm. Biomed. Sci*. **2013**, 35, 1732–8.
15. Bayram, HM, Arda Ozturkcan, S.; *J. Funct. Foods*, **2020**, *75*, 104252.
16. Uncini Manganelli RE, Zaccaro L, Tomei PE. *J. Ethnopharmacol*. **2005**, *98*,23–7.
17. Fazio A, Plastina P, Meijerink J, Witkamp RF, Gabriele B. *Food Chem*. **2013**, *140*, 817–24.
18. Lee J, Finn CE. *J. Sci. Food Agric*. **2007**, *87*, 2665–75.
19. Dawidowicz AL, Wianowska D, Baraniak B. *LWT - Food Sci.Technol*. **2006**, *39*, 308–15.
20. Arceusz A, Wesolowski M. *Open Chem*. **2015**,*13*, 1196–208.
21. Ferreira-Santos, P; Badim, H; Salvador, ÂC; Silvestre, AJD; Santos, SAO; Rocha, SM; Sousa, AM; Pereira, MO; Wilson, CP; Rocha, CMR, Teixeira JA, Botelho C. *Biomolecules*. **2021**, 11.
22. Matyas M, Hasmasanu MG, Zaharie G. *Medicina* **2019**, *55*, 720.
23. Liu H, Pierre-Pierre N, Huo Q. *Gold Bull*. **2012**, *45*, 187–95.
24. Pokrowiecki R, Wojnarowicz J, Zareba T, Koltsov I, Lojkowski W, Tyski S, Mielczarek A, Zawadzki P.; *Int. J. Nanomed*. **2019**, *14*, 9235-9257.
25. Sohal IS, Cho YK, O'Fallon KS, Gaines P, Demokritou P, Bello D. *ACS Nano*. **2018**, *12*, 8115–28.
26. Mikulic-Petkovsek M, Samoticha J, Eler K, Stampar F, Veberic R. *J. Agric. Food Chem*. **2015**, *63*, 1477–87.
27. Moldovan R, Mitrea DR, Florea A, Chiş IC, Suciu Ş, David L, Moldovan BE, Mureşan LE, Lenghel M, Ungur RA, Opris RV, Decea N, Clichici SV; *Antioxidants* (Basel). **2022**, *11*, 1343.
28. Baldea I, Florea A, Olteanu D, Clichici S, David L, Moldovan B, Cenariu M, Achim M, Suharoschi R, Danescu S, Vulcu A, Filip GA; *Nanomedicine* (*Lond*). **2020**, *15*, 55-75.

29. Minekus M, Alminger M, Alvito P, Ballance S, Bohn T, Bourlieu C, Carrière F, Boutrou R, Corredig M, Dupont D, Dufour C, Egger L, Golding M, Karakaya S, Kirkhus B, Le Feunteun S, Lesmes U, Macierzanka A, Mackie A, Marze S, McClements DJ, Ménard O, Recio I, Santos CN, Singh RP, Vegarud GE, Wickham MS, Weitschies W, Brodkorb A. *Food Funct*. **2014**, 5.
30. Janaszewska A, Bartosz G., *Scand. J. Clin. Lab. Invest*. **2002**, *62*, 231–6.
31. Singleton VL, Orthofer R, Lamuela-Raventós RM. *Methods Enzymol*. **1999**, *299*, 152–78.
32. Perde-Schrepler M, David L, Olenic L, Potara M, Fischer-Fodor E, Virag P, Imre-Lucaci F, Brie I, Florea A, *J. Nanomater.* **2016**, 6986370.